

Supplementary Material

Programmable Shape Transformation of Elastic Spherical Domes

Arif M. Abdullah^a, Paul V. Braun^{a,b,c}, and K. Jimmy Hsia^{a,b,d*}

^a Department of Mechanical Science and Engineering, University of Illinois at Urbana–Champaign, Urbana, IL 61801

^b Frederick Seitz Materials Research Laboratory, University of Illinois at Urbana–Champaign, Urbana, IL 61801

^c Department of Materials Science and Engineering, University of Illinois at Urbana–Champaign, Urbana, IL 61801

^d Departments of Mechanical Engineering and Biomedical Engineering, Carnegie Mellon University, Pittsburgh, PA 15213

*To whom correspondence may be addressed. Email: kjhsia@cmu.edu

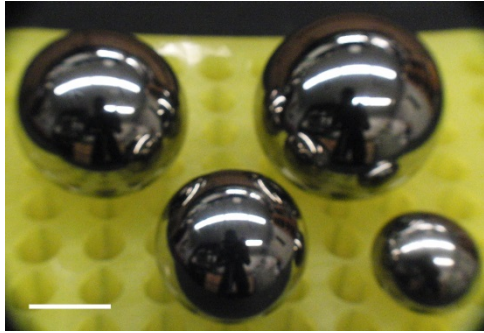
Movie S.1: Mismatch strain driven shape transformation of a bilayer spherical dome with $\frac{r}{t} = 50$ and $\frac{r\theta}{t} = 45$. This movie corresponds to Figure 4 of the main text.

Movie S.2: Mismatch strain driven shape transformation of a bilayer spherical dome with $\frac{r}{t} = 50$ and $\frac{r\theta}{t} = 30$. This movie corresponds to Figure S.2 of the Supplementary Material.

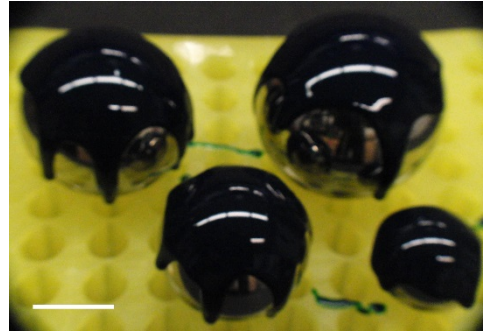
Movie S.3: Mismatch strain driven shape transformation of a bilayer spherical dome with $\frac{r}{t} = 50$ and $\frac{r\theta}{t} = 100$. This movie corresponds to Figure S.3 of the Supplementary Material.

Movie S.4: Experimental demonstration of the bilayer dome shape transformation behavior with increasing mismatch strain. Dome 1, shown at the right of the screen is smaller and weakly curved ($\frac{r}{t} = 559.3$ and $\frac{r\theta}{t} = 428.8$) compared to bigger and strongly curved dome 2 ($\frac{r}{t} = 459.4$ and $\frac{r\theta}{t} = 548.8$).

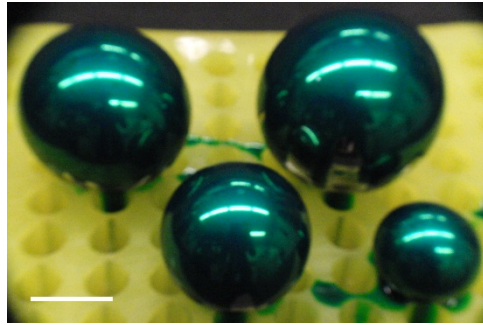
Movie S.5: Experimental demonstration of the bilayer dome response with decreasing mismatch strain. Dome 1, shown at the right of the screen is smaller and weakly curved ($\frac{r}{t} = 559.3$ and $\frac{r\theta}{t} = 428.8$) compared to bigger and strongly curved dome 2 ($\frac{r}{t} = 459.4$ and $\frac{r\theta}{t} = 548.8$).



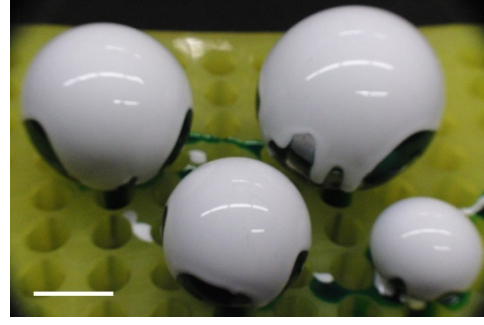
(a) Chrome steel balls of different sizes



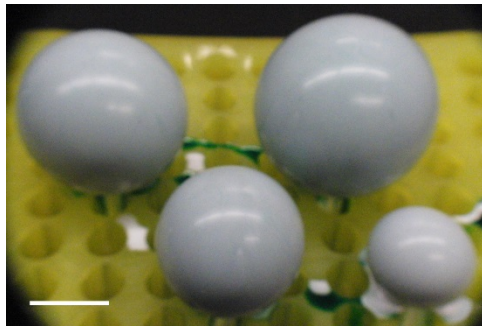
(b) Green pigmented PDMS is poured



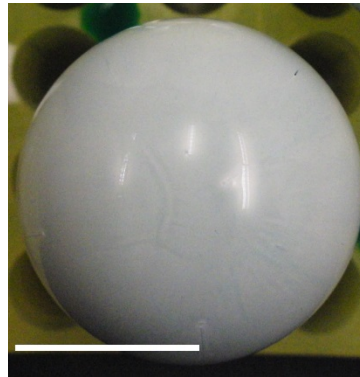
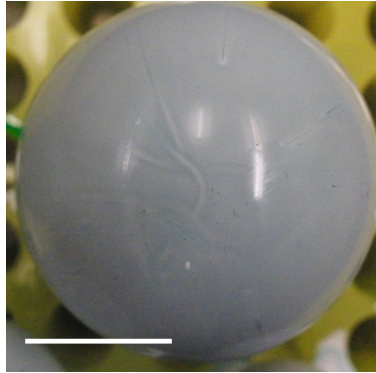
(c) Partially cured inner layer



(d) White pigmented PDMS is poured



(e) Fully cured bilayers on chrome steel balls, which could be cut into domes using hollow punches (shown in Figure 2 of the main text.)



(f) Surface imperfections on fabricated bilayers

Figure S.1: (a) to (e) demonstrate the step by step dome fabrication procedure. (f) shows point-like and striation marks on dome surfaces. Scale bar size is 20 mm.

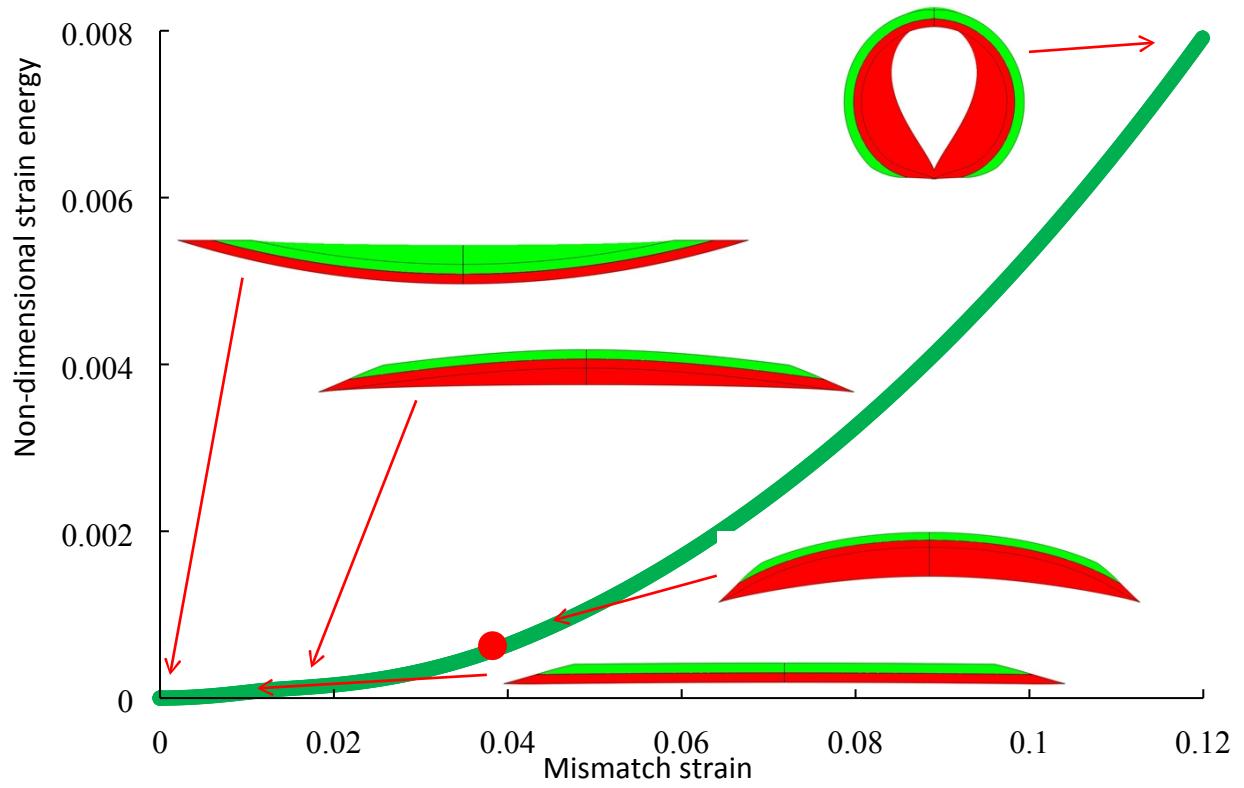
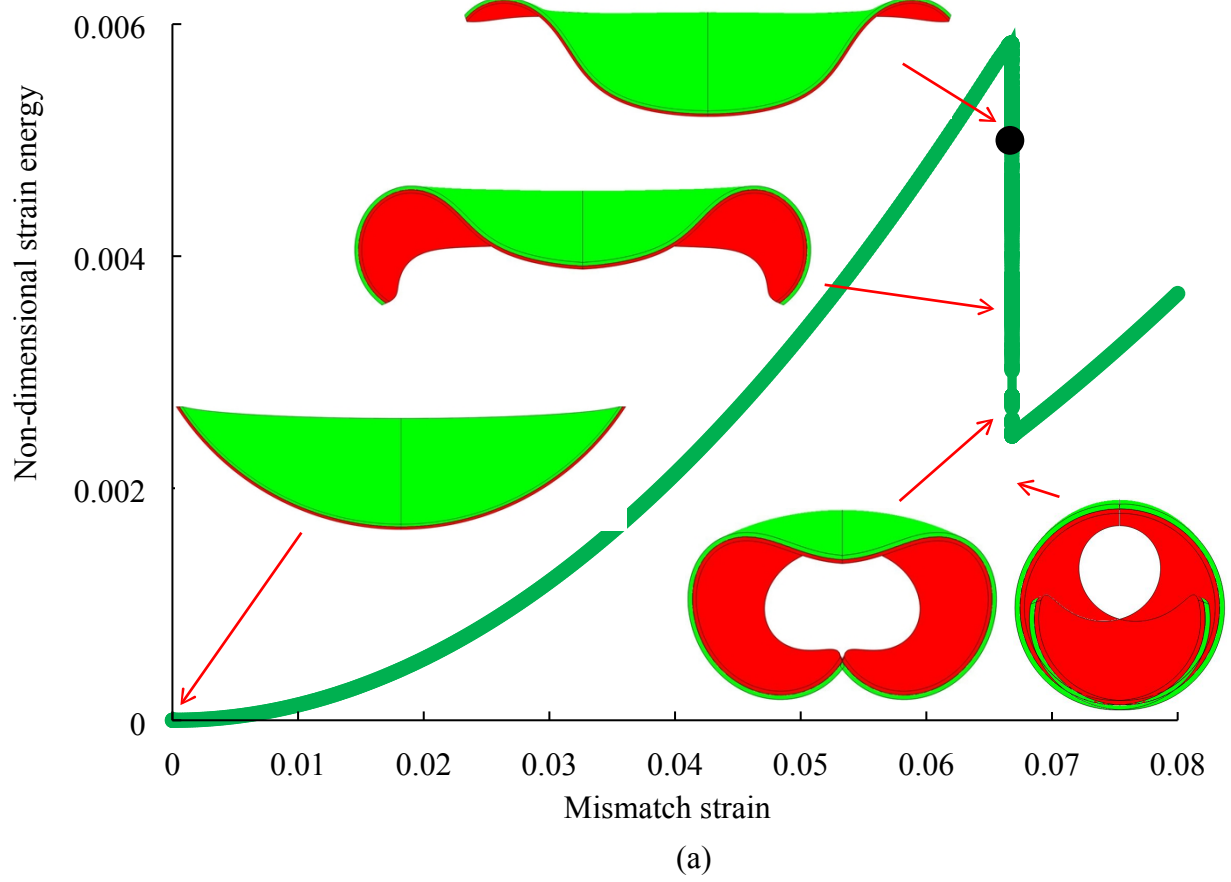


Figure S.2: Strain energy – mismatch strain scenario for a dome with $\frac{r}{t} = 50$ and $\frac{r\theta}{t} = 30$. There is no snap-through for this particular geometry and the red dot denotes bifurcation buckling.



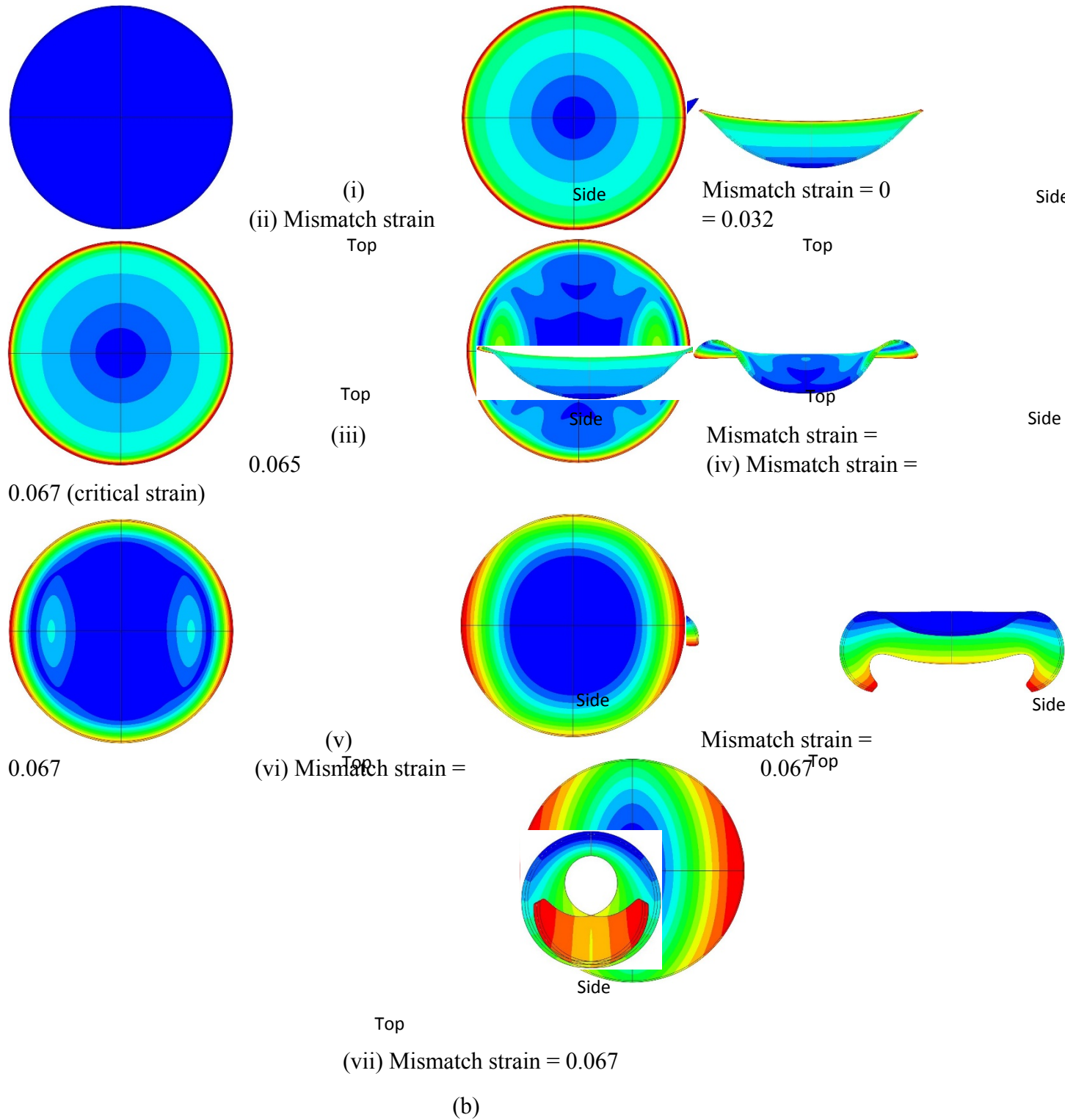


Figure S.3: (a) Strain energy – mismatch strain scenario for a dome with $\frac{r}{t} = 50$ and $\frac{r\theta}{t} = 100$.

All three deformation modes: snap-through, bifurcation buckling and subsequent morphing into a cylinder initiate at the black dot for this particular geometry. (b) Displacement contours (blue

means low and red means high) plotted on the original (top view) and deformed (side view) dome geometries at different mismatch strain levels. Snap-through, Bifurcation buckling and morphing into a full cylinder occur at the critical mismatch strain value of 0.067.

Applied mismatch strain

Simulation time

(a)

Applied mismatch strain

Experiment time

(b)

Figure S.4: Mismatch strain application schemes adopted for finite element simulations (a) and experiments (b).

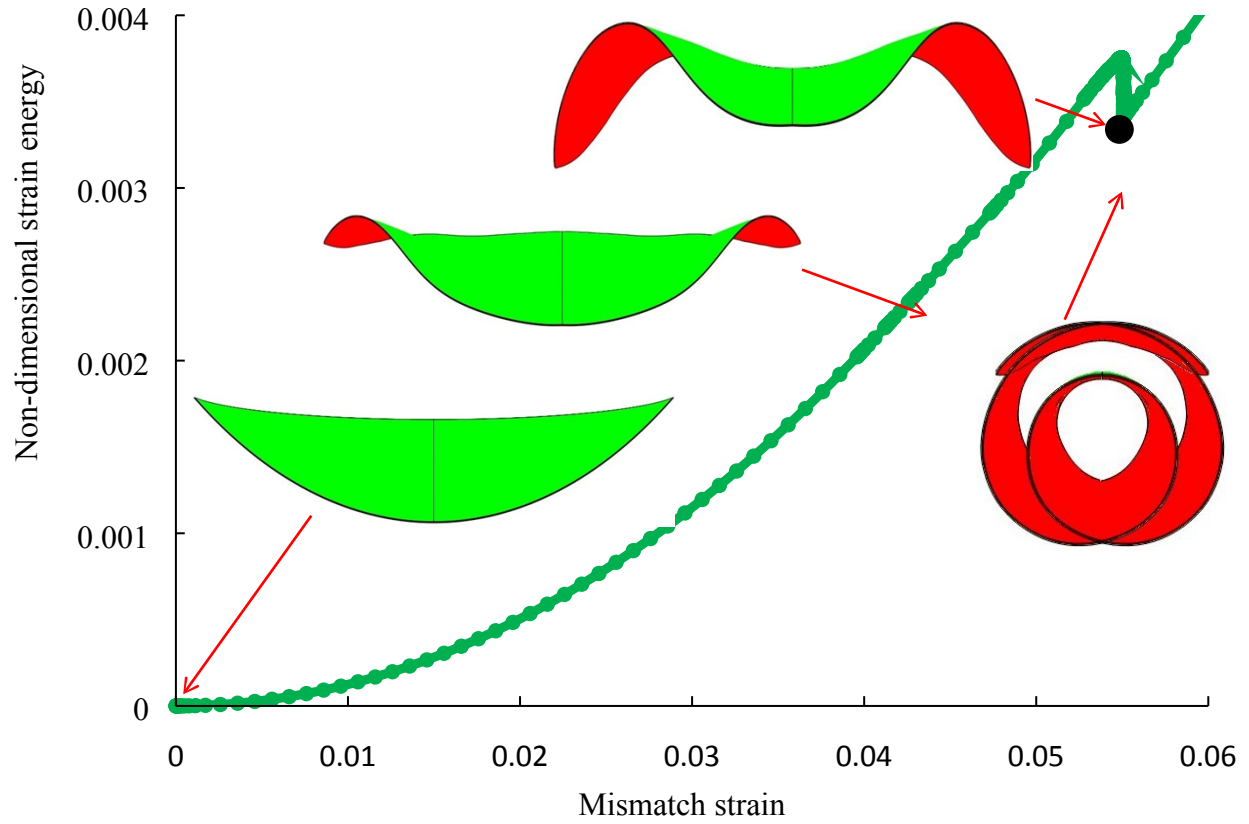


Figure S.5: Strain energy – mismatch strain scenario for an experimental dome sample with $\frac{r}{t} = 525$ and $\frac{r\theta}{t} = 653$. The shear and bulk modulus for the inner layer are 0.186 MPa and 739 MPa and those for the outer layer are 0.42 MPa and 1215 MPa⁴⁰. All three deformation modes: snap-through, bifurcation buckling and subsequent morphing into a cylinder initiate at the black dot for this particular geometry.

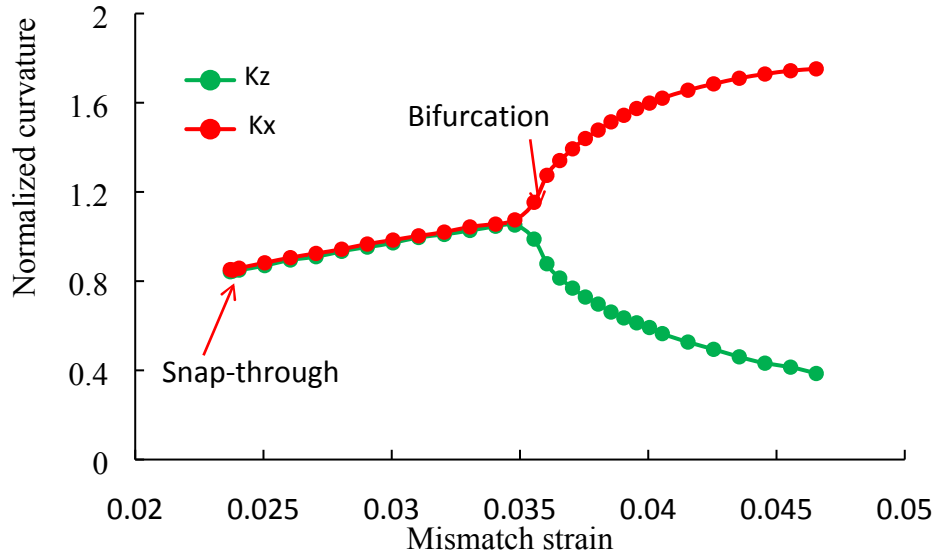
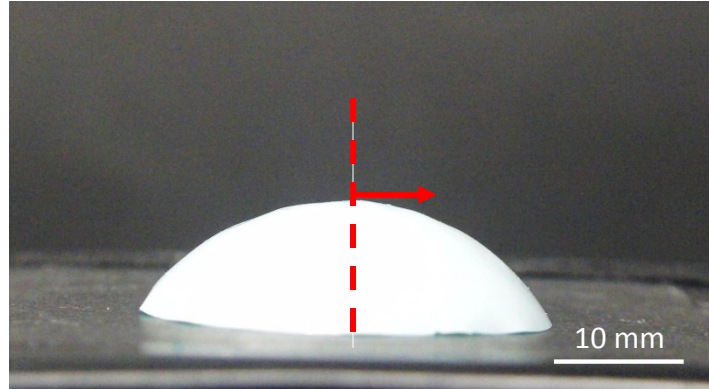


Figure S.6: Normalized principle curvature vs. mismatch strain plot for a group 1 dome ($\frac{r}{t} = 50$ and $\frac{r\theta}{t} = 45$) beyond snap-through. Absolute values of principal curvature (K_z and K_x) after inversion have been normalized by the dome initial curvature.



(a) Bilayer dome with an arrow showing the direction along which sections are cut

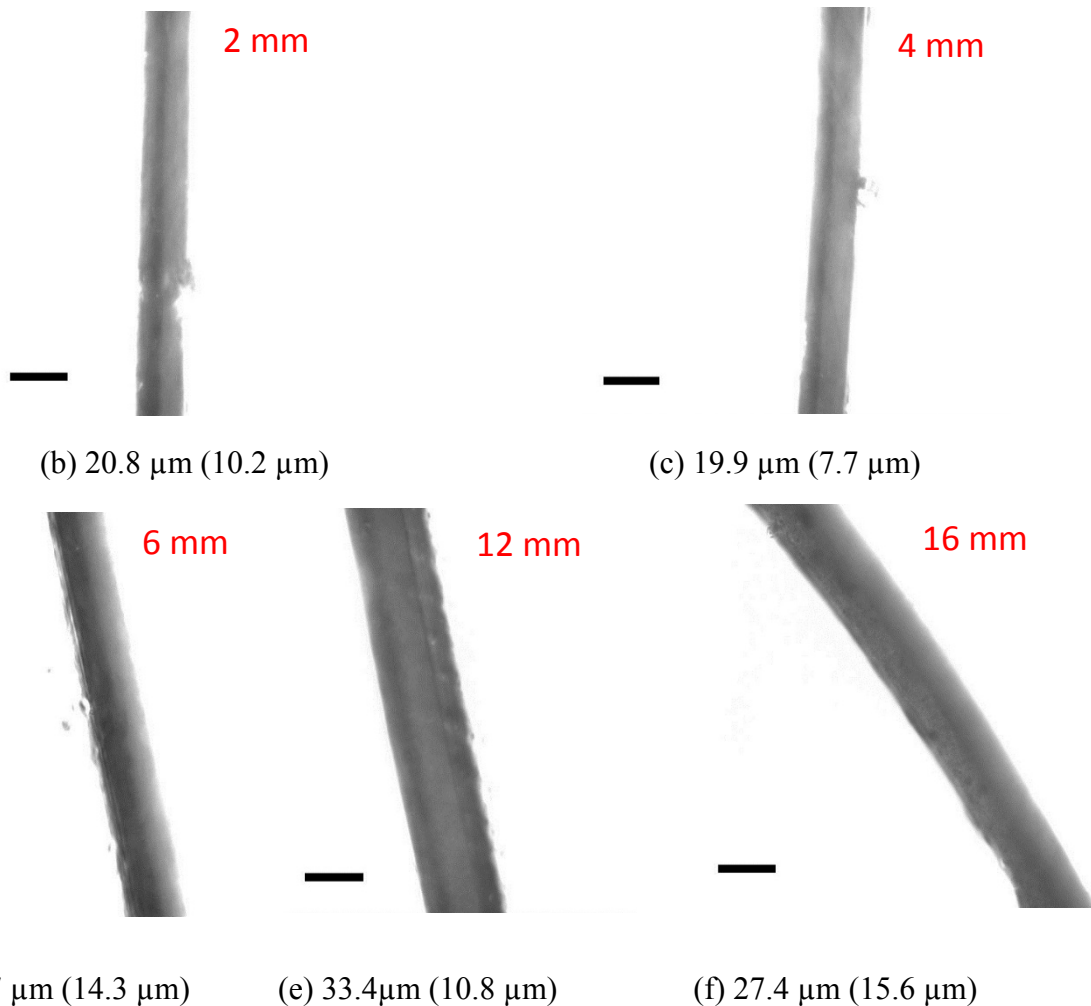


Figure S.7: (a) A bilayer dome from which sections are cut at different distances for thickness measurement. (b) to (f) shows cross-sectional images of the cut sections (darker shade represents the green inner layer) at 2, 4, 6, 12 and 16 mm from the central red line in (a). The corresponding measured thickness values are included in the label with their inner layer counterpart written inside the parenthesis. Scale bar size for (b) to (f) is 25 micron.

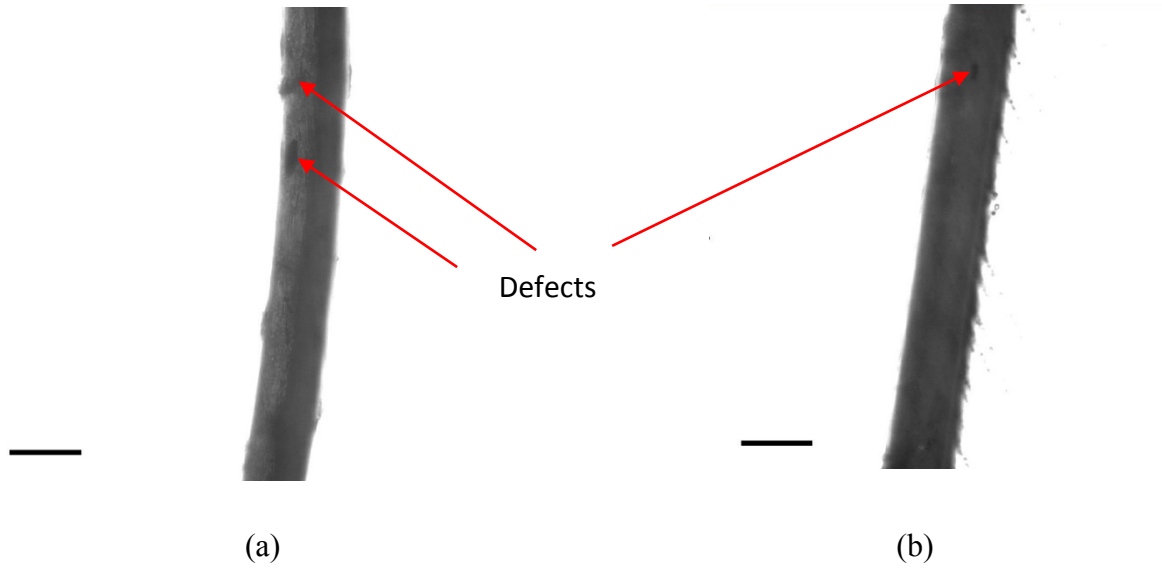


Figure S.8: (a), (b) shows through thickness defects in two different bilayer dome cross sections. Scale bar size is 50 micron.